Shear instability of two-fluid parallel flow in a Hele–Shaw cell

P. Gondret and M. Rabaud
Laboratoire Fluides, Automatique et Systèmes Thermiques, Universités P. & M. Curie et Paris-Sud et CNRS (URA 871), Bât. 502, Campus Universitaire, F-91405 Orsay Cedex, France

(Received 20 May 1997; accepted 24 July 1997)

We study experimentally the parallel flow in a Hele–Shaw cell of two immiscible fluids, a gas and a viscous liquid, driven by a given pressure gradient. We observe that the interface is destabilized above a critical value of the gas flow and that waves grow and propagate along the cell. The experimental threshold corresponds to a velocity difference of the two fluids in good agreement with the inviscid Kelvin–Helmholtz instability, while the wave velocity corresponds to a pure viscous theory deriving from Darcy's law. We report our experimental results and analyze this instability by the study of a new equation where the viscous effects are added to the Euler equation through a unique drag term. The predictions made from the linear stability analysis of this equation agree with the experimental measurements. © *1997 American Institute of Physics.* [S1070-6631(97)04211-6]

I. INTRODUCTION

Among the long list of hydrodynamic instabilities, one of the classical teaching examples is the Kelvin–Helmholtz instability which affects an interface submitted to a shear. It is the paradigm of a shear instability: When two layers of fluids move at different velocities, their interface could be unstable by the effect of inertia. A linear analysis of the instability can be found in various text book, for example in Chandrasekhar's.[1] The appearance of waves at the sea surface under the wind action is ascribed to this instability. However, experimental results are not in agreement with the simplest theoretical predictions as they predict waves only for very high winds.[2] Usually the linear analysis is nonviscous and corresponds to a two-dimensional parallel basic flow which is homogeneous in space. This last condition is the most difficult to realize experimentally and the basic flow corresponds usually to a ''free mixing layer configuration'' where two layers of fluids flow in the same direction but with different velocities at the end of a splitting plate. Thus the basic profile enlarges downward by the diffusion of the boundary layers, and both spatial and temporal evolutions of initial perturbations are then irremediably coupled. It is only in particular set-ups that this difference between simple models and real profiles could be, partially, overtaken. For example the basic shear profile can be made homogeneous in space, either in linear geometry with contrary flowing fluids[3,4] or in circular geometry.[5,6] In the first case the price to pay is that the basic flow is not stationary but evolves in time; thus, no stable solutions of the instability can be observed. In the second case the cells are periodic and closed; quantification effects can be important and the dynamic is no more then one of an open system. Stationary unstable states could be achieved but temporal evolution of perturbations is difficult to study.

In the present paper we present a new experimental set-up where a spatially uniform and time independent shear flow is forced in an open geometry. In our confined Hele–Shaw configuration, the diffusive layers have exactly the same extension on either side of the interface whatever the distance from the entrance and even though the viscosities of the two fluids are much different.[7] This extension is equal to the gap of the cell and the basic velocity profile is thus constant in time and space. Here the price to pay is that viscosity is no more negligible and a new linear analysis must be developed.

The rest of the paper is organized as follows. In Sec. II we present the experimental set-up and experimental results about the instability threshold. In Sec. III a new linear analysis, taking into account the viscous friction on the walls, is presented. Its predictions are favourably compared to experimental results.

II. EXPERIMENT

A. Experimental set-up

We have studied the parallel flow of two immiscible fluids, a liquid and a gas, in a Hele–Shaw cell.[8] A schematic view of the experimental set-up is shown in Fig. 1. The cell is made of two glass plates (22 mm thick) separated by a thin sheet of mylar (thickness $e=0.35$ mm) in which a cavity of height $h=10$ cm and length $L=120$ cm is delimited for the fluid flow. The mylar sheet ensures the tightness and a constant gap. The cell is located so that the gravity $\mathbf{g}$ is in the plane of the cell and perpendicular to the length L of the cell. The gas is nitrogen of viscosity $\mu_{N_2}=17.5\times10^{-6}$ Pa s. The gas being contained in a high pressure bottle (20×10^6 Pa), we use a relief valve to adjust the injection over pressure in the range $[0,10^4]$ Pa. This pressure is controlled by a manometer and the flow rate is measured by a ball debimeter. Typical flow rate is of the order of 10^{-4} m^3/s. The liquid we used is a silicon oil (Rhodorsil V100, Rhône-Poulenc) of viscosity $\mu_{\mathrm{oil}}=0.1$ Pa s, density $\rho_{\mathrm{oil}}=965$ kg m^{-3} and interfacial tension $\gamma=20.6\times10^{-3}$ N/m. The silicon oil wets the glass plates very well; so is the interface regular, horizontal, and well defined. When the cell is illuminated from behind, the interface appears as a black line because of the transverse curvature of the meniscus. This allows an easy visualization and the interface position is recorded and analyzed by video means. The two fluids enter separately in the cell with the gas above the liquid but at the same pressure $P_{\mathrm{in}}=P_0+\Delta P$ at each side of the interface and go out the cell also separately and at the same pressure P_0. The control parameter of

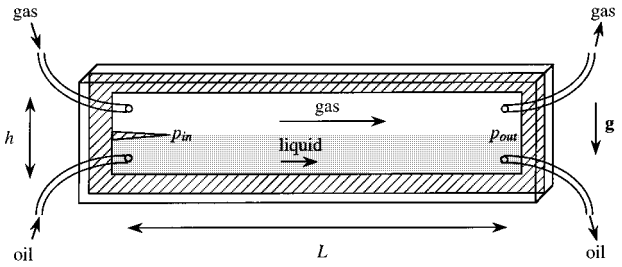

FIG. 1. Experimental set-up. The two glass plates are separated by a mylar sheet (hatching) of thickness $e=0.350$ mm. The distance between the entrance and the exit is $L=120$ cm, the height is $h=10$ cm. The two fluids enter in the cell at the same pressure $P_{\text{in}}\approx 1.1\times 10^5$ Pa and go out at the same pressure $P_{\text{out}}=10^5$ Pa. The interface between the liquid and the gas is horizontal at any time below the instability threshold.

the experiment is the injection over pressure ΔP. Below the instability threshold, the two fluids flow parallel at different velocities with an horizontal interface, the velocity ratio being equal to the inverse of the viscosity ratio as shown in Darcy's law presented hereafter. Thus a strong shear exists at the interface. Note that, as could be noticed in Fig. 1, the two fluids are not in contact immediately at their entrance in the cell but after a slight tongue of 10 cm likewise the splitter plate in classical mixing layers set-ups. The interface position can be modulated locally (at the end of the tongue) by a periodic modulation of the oil injection pressure. This is done by a periodic opening and closing of an electrovalve located on a small tube in parallel with the main feed tube of liquid. The electrovalve is controlled by a signal generator at a low frequency ($f\approx 0.1$ Hz). This set-up allows us to study the response of the system at a well defined frequency. The square modulation of pressure is smoothed by the flexible tubes and we check that the modulation of the interface position is rather sinusoidal at the entrance of the cell. The interface modulation in position is chosen to be typically 1 mm peak to peak which corresponds to a pressure modulation of 10 Pa, and thus to a perturbation of 1% of the injection pressure.

In the lubrication approximation, the flow of the two fluids is governed in a Hele–Shaw cell by Darcy's law[9] for the transverse averaged velocity:

$$u(x)=-\frac{e^2}{12\mu}\frac{\partial P}{\partial x}.$$

In the incompressible case, $(\nabla.\mathbf{u}=0)$ and for a flat interface the velocity of each fluid is constant along the cell. Thus, the local pressure gradient $\partial P/\partial x$ is also constant. The pressure decreases linearly along the flow direction: $P(x)=(P_{\text{out}}-P_{\text{in}})/Lx+P_{\text{in}}$. The pressure gradient being the same for the two fluids, their velocities U_{gas} and U_{liq} are linked by the relation $\mu_{\text{gas}}U_{\text{gas}}=\mu_{\text{liq}}U_{\text{liq}}$.

As gas is a compressible fluid, we have estimated the possible deviation induced by the compressibility. Indeed, the gas velocity increases typically of an amount of 10% from the entrance to the exit because of the expansion of the gas. This result is observed close to the instability threshold without the forcing set-up as waves appears first at the end of the cell. The second effect is that the pressure decrease is not

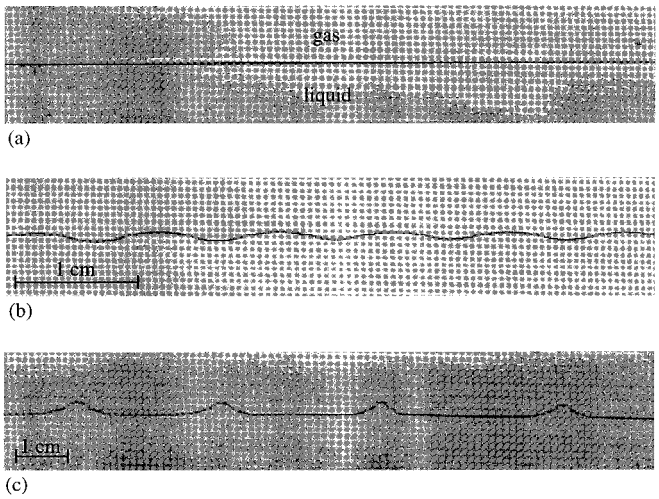

FIG. 2. Interface between the gas and the liquid in the Hele–Shaw cell at increasing flow rates. (a): flat interface; (b): linear waves; (c): localized waves. Waves propagate along the flow direction from left to right.

perfectly linear but slightly curved. This deforms slightly the interface which goes downward roughly linearly almost all along the cell with a maximum deviation of 2 mm near the end of the cell. We are not annoyed by this effect.

The typical Reynolds number of the flow when evaluated with the thickness e of the cell is 10^2 for the gas and 3×10^{-3} for the liquid. In porous media, it is experimentally found that Darcy's law does not hold at Reynolds numbers larger than a critical value ranging between 1 and 10, this spread being due to the uncertainty of the typical pore size.[10] One must then add higher order terms to take into account the inertia terms. These terms come into play because of the non-parallel nature of the flow at the connections between pores. In a Hele–Shaw cell, these problems arising from the pore distribution and from the tridimensional nature of the flow can be ignored. The inertia terms are strictly zero as long as the flow remains unidirectional and Darcy's law still holds at much larger Reynolds numbers. Indeed, the critical Reynolds number corresponding to the laminar-turbulent transition is known to be equal to 5772 in plane Poiseuille flow[11] and is also known to increase monotonically in a square duct of decreasing aspect ratio from infinity to one, the flow being considered to be stabilized by the presence of endwalls.[12]

B. Experimental results

1. Interface visualization and qualitative description of the instability

We will now describe the aspect of the interface when increasing the injection pressure. Without forcing set-up, the interface is horizontal and stable at low shear (Fig. 2(a)). At a given injection pressure, it becomes unstable and one can observe few sinusoidal propagating waves with a wavelength of order 1 cm which grow somewhere in the cell (Fig. 2(b)). These linear waves evolve rapidly into localized waves (Fig. 2(c)). These solitary waves are roughly 3 mm height and 3 mm width and separated by a distance of few centimeters. They propagate steadily, much more faster than the previous

sinusoidal waves. At larger flow rates, the solitary waves begin to interact with a complex scenario. At even larger velocity differences, the interface becomes more and more disordered with small crests on big crests and emission of drops occurs. Finally, a diphasic flow is obtained. Without local forcing, the transition is quite abrupt and the linear waves are transient and hence difficult to study. Otherwise, the solitary waves are not regularly spaced.

Note that all these observations are not dependant on the precise height of the interface, as long as this height is not smaller than the thickness of the cell, i.e., typically one millimeter. Hence, by contrast with the Poiseuille or Couette parallel flow of two fluids in rectangular or circular ducts[6,13] or with the gas flow over a thin liquid film,[14] the liquid height is not a relevant parameter of this experiment.

2. Experimental measurements

As the interfacial pattern evolves rapidly above threshold, we study the response of the interface to a periodically imposed perturbation of the injection pressure for the liquid. As we activate our local forcing set-up, we observe the same threshold and the same general scenario. The local pressure perturbation induces a small harmonic deformation of the interface (typically 1 mm peak to peak) at the end of the separating tongue, and we observe if this interfacial deformation is amplified or damped when propagating. Above the threshold, the linear waves are amplified and evolve into periodic localized waves. The injection pressure above which the perturbations is amplified is recorded as the threshold. This corresponds to a velocity of $U_{c_{\mathrm{gas}}}=4.62$ m/s for the gas, which is very close to the one predicted by the Kelvin–Helmholtz (KH) linear analysis ($\Delta U_{\min_{\mathrm{KH}}}=4.67$ m/s). This result is in agreement with the known paradox that inviscid KH theory predicts much better the threshold in the case of the wind flow over a high viscous liquid that over water.[15] The KH analysis which is recalled in Sec. III A. predicts a gravity dependence of the velocity threshold with a power law of $g^{1/4}$ (Eq. (7)). This dependence is difficult to test in classical wind-waves set-ups but here we can easily study it by tilting the plane of the cell. The apparent in plane gravity is then $g=g_0 \sin\theta$, where θ is the angle between the cell plane and the horizontal plane. The transverse component of **g** induces only a small asymmetry of the meniscus. Indeed, this asymmetry remains small as long as the thickness is small compared to the capillary length. The velocity threshold as a function of the normalized gravity g/g_0 is shown in Fig. 3. The experimental threshold decreases as the apparent gravity decreases. Note that at very small angle ($\theta<3°$) any deformation of the interface relaxes very slowly and it is very difficult to conclude if initial perturbations are amplified or damped. However, the agreement between the measurements and the KH predictions is very good.

We can modify the forcing frequency and then force different wave-numbers. The instability threshold as a function of the wave-number is shown in Fig. 4. The minimum value is obtained for $k\approx 575\ \mathrm{m}^{-1}$ ($\lambda\approx 1.05$ cm) which is a little bit smaller than the corresponding capillary length k_c $=677\ \mathrm{m}^{-1}$. Below the value $k=375\ \mathrm{m}^{-1}$ no measurements are reported as it is the first harmonic of the forcing that is amplified.

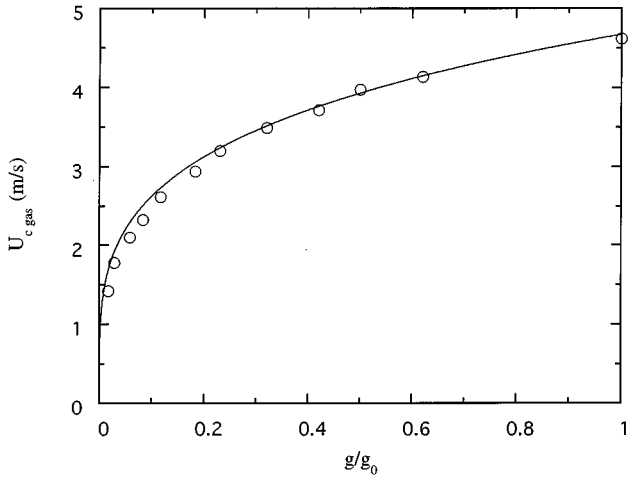

FIG. 3. Gas velocity at the onset of instability, $U_{c_{\mathrm{gas}}}$, as a function of the normalized apparent gravity g/g_0. Experimental results (○) and Kelvin–Helmholtz prediction (solid line).

The determination of the threshold can be more precise by measuring the damping length. Below the instability threshold, the harmonic perturbation of the interface propagates but is damped. We measure the increase of the damping length Λ as the threshold is approached (Fig. 5). The extrapolation of a linear fit of $1/\Lambda$ gives the value $U_{c_{\mathrm{gas}}}=4.72$ m/s in agreement with the previous visual determination. The slope of this linear fit is $\alpha=0.2\pm 0.02\ \mathrm{m}^{-1}$. This leads to the growth rate $\sigma=\alpha(U_{\mathrm{gas}}-U_{c_{\mathrm{gas}}})\approx 0.06\ \mathrm{s}^{-1}$ for the gas velocity $U_{\mathrm{gas}}=5$ m/s. This value is roughly three order of magnitude smaller than the one predicted by KH theory ($\sigma_{\mathrm{KH}}=50\ \mathrm{s}^{-1}$).

The waves are propagating with a non-zero velocity even at the threshold. We measured the wave velocity by

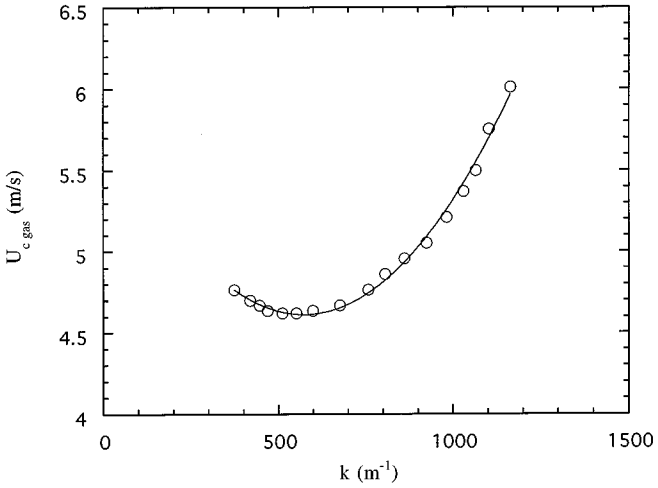

FIG. 4. Velocity threshold $U_{c_{\mathrm{gas}}}$ as a function of wave-number k. The solid line is a parabolic fit through the experimental data (○).

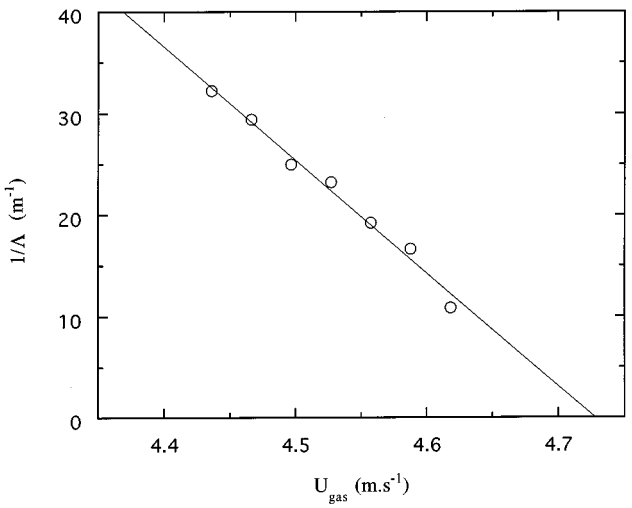

FIG. 5. Inverse of the damping length Λ vs the gas velocity U_{gas}. The solid line is a linear fit through the experimental data (○).

measuring the wavelength λ and knowing the forcing frequency f. At the threshold, we found a wave velocity of $V_\varphi = 1$ mm/s. This value is several times smaller than the one predicted by KH ($c_{r_{\text{KH}}} = 7$ mm/s).

Furthermore, amplitude and wave measurements above threshold (to be reported elsewhere) have convinced us that the instability corresponds to a Hopf bifurcation. However, the dilemma arising from the excellent agreement between experimental measurements and KH predictions for the threshold and bad ones for the wave velocity and for the growth rate was a strong stimulation to revisit this analysis. In the next section, we develop a new linear analysis more suitable to our configuration.

III. LINEAR STABILITY ANALYSIS

Let us consider the bidimensional parallel flow of two fluids of different velocities U_1 and U_2 along x direction, of different densities ρ_1 and $\rho_2 = \rho_1 + \Delta\rho (\Delta\rho > 0)$ with the lighter above, and of different viscosities μ_1 and μ_2 (Fig. 6). The interface is horizontal and flat at $y = 0$. The gravity $\mathbf{g}$ is perpendicular to the interface along y direction and the interfacial surface tension between the two fluids is γ. Note

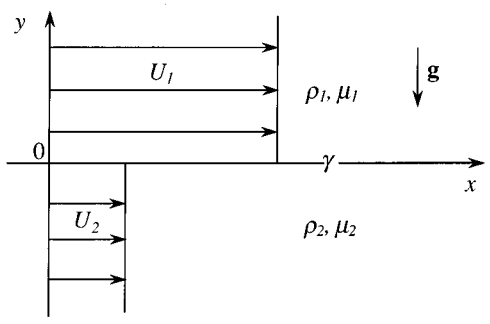

FIG. 6. Sketch of the parallel flow of two fluids flowing respectively with velocity U_1 and U_2, of densities ρ_1 and $\rho_2 (\rho_2 > \rho_1)$, of viscosities μ_1 and μ_2 and of interfacial tension γ.

that we do not consider the two walls up and down. This is correct as long as the wavelength is much smaller than the distance between the interface and the walls.

From the Navier–Stokes equation, one can usually derive two equations in two limiting cases. In one limiting case, one can neglect the viscosity terms, and the Navier–Stokes equation reduces to the Euler equation. In another limiting case, one can neglect the inertial and unstationary terms, and the Navier–Stokes equation reduces to Stokes equation or to Darcy's equation if the flow is confined in a Hele–Shaw cell. In the first section, we recall the classical results of the stability analysis of this flow governed by the Euler equation, known as the Kelvin–Helmholtz theory. In the second section, we present the linear stability analysis given by the Darcy equation following the work of Zeybek and Yortsos[16,17] but adding the effect of gravity. At last, in the third section, we present a new equation taking into account some terms of the two previous equations and we perform the linear stability analysis of this new equation.

A. Pure inviscid case (Kelvin–Helmholtz theory)

For inviscid fluids, the Navier–Stokes equation reduces to the Euler equation:

$$\frac{\partial \mathbf{u}}{\partial t} + (\mathbf{u}.\nabla)\mathbf{u} = -\frac{1}{\rho}\nabla p. \tag{1}$$

For our two-dimensional problem in the (x,y) plane of the cell, it is convenient to introduce the stream function ψ ($u = \partial\psi/\partial y$ and $v = -\partial\psi/\partial x$) and the equation reduces to:

$$\frac{\partial \Delta\psi}{\partial t} + (\mathbf{u}.\nabla)\Delta\psi = 0. \tag{2}$$

Small perturbations of the form $\phi(y)\exp[ik(x-ct)]$ superimposed to the basic stationary and unidirectional flow of velocity profile $U_0(y)$ along x direction are governed by the Rayleigh equation:

$$(U_0 - c)\left(\frac{d^2\phi}{dy^2} - k^2\phi\right) - \frac{d^2U_0}{dy^2}\phi = 0, \tag{3}$$

where k is the real wave-number and c the complex phase velocity.

We now choose $U_0(y)$ to be discontinuous at the interface between the two fluids (Fig. 6). Note that in our geometry, the profile is continuous on a scale equal to the thickness of the cell.[7] However, as long as the wavelength is much larger than the thickness (and this is the case in the experiments), the profile may be considered as discontinuous.[1] Solving the Rayleigh equation and imposing the usual continuity of displacement at the interface $y = 0$, the jump condition for the pressure at the interface due to surface tension and the exponential decays at $y = \pm\infty$ leads to the following classical dispersion relation:

$$c^2 - 2\frac{\rho_1 U_1 + \rho_2 U_2}{\rho_1 + \rho_2}c + \frac{\rho_1 U_1^2 + \rho_2 U_2^2}{\rho_1 + \rho_2} - \frac{\Delta\rho g + \gamma k^2}{(\rho_1 + \rho_2)k} = 0. \tag{4}$$

The solutions are

$$c=c_r+ic_i=\frac{\rho_1U_1+\rho_2U_2}{\rho_1+\rho_2}\pm i\left[\frac{\rho_1\rho_2}{(\rho_1+\rho_2)^2}(U_1-U_2)^2-\frac{\Delta\rho g+\gamma k^2}{(\rho_1+\rho_2)k}\right]^{1/2}, \quad (5)$$

where c_r is the phase velocity of the waves and $\sigma=kc_i$ the temporal growth rate of the waves. The wave velocity appears here as the mean, weighted by the densities, of the two fluid velocities. In the imaginary part of the velocity appears the balance between the destabilizing term of inertia and the stabilizing terms of gravity and surface tension for respectively long and short waves. The condition for the velocity difference $\Delta U=U_1-U_2$ at which waves grow is

$$\Delta U^2\geqslant\frac{\rho_1+\rho_2}{\rho_1\rho_2}\left(\Delta\rho\frac{g}{k}+\gamma k\right). \quad (6)$$

The minimum is for the critical wave-number $k_c=1/l_c$, where $l_c=(\gamma/(\Delta\rho g))^{1/2}$ is the capillary length. The corresponding minimum velocity threshold is then

$$\Delta U_{\min}=\left[\frac{2(\rho_1+\rho_2)}{\rho_1\rho_2}(\Delta\rho g\gamma)^{1/2}\right]^{1/2}. \quad (7)$$

For $\Delta U\geqslant\Delta U_{\min}$, the unstable waves are those of wavenumbers in a range containing k_c and of extrema

$$k_{\max/\min}=\frac{\rho_1\rho_2}{2(\rho_1+\rho_2)\gamma}\Delta U^2\pm\left[\left(\frac{\rho_1\rho_2}{2(\rho_1+\rho_2)\gamma}\Delta U^2\right)^2-\frac{\Delta\rho g}{\gamma}\right]^{1/2}. \quad (8)$$

B. Pure viscous case (Darcy's law)

For pure viscous fluids, the Navier–Stokes equation reduces to the Darcy equation in the case of a bidimensional flow in a Hele–Shaw cell of thickness e:

$$\mathbf{u}=(u,v)=-\frac{e^2}{12\mu}\nabla p, \quad (9)$$

where $\mathbf{u}$ is the gap-averaged velocity. Indeed, a narrow-gap assumption leads to the conclusion that the pressure is independent of the transverse direction z and that the velocity in the fluids is everywhere in the direction of the pressure gradient, varying in a parabolic manner between the planes.[18] This allows the velocity to be averaged over the gap to remove the dependence on z. The x and y component of this averaged velocity, u and v, are given by Eq. (9). Note that this analysis can be expected to hold only up to distances of order e from the interface and likewise the parabolic velocity distribution across the gap. From Darcy equation (Eq. (9)), it follows that, the pressure gradient being identical for the two fluids, their velocities are related by $\mu_1U_1=\mu_2U_2$. Assuming the incompressibility of the two fluids leads to Laplace equation for the pressure: $\Delta p=0$. We then followed the linear stability analysis performed by Zeybek and Yortsos[16,17] in the case of parallel flow in Hele–Shaw cell but adding the effect of gravity. Assuming small perturbations of the form $p(y)\exp[ik(x-ct)]$ for the pressure superimposed to the basic stationary and unidirectional flow along x direction and imposing the usual continuity of displacement at the interface $y=0$, the jump condition for the pressure at the interface due to surface tension and the exponential decays at $y=\pm\infty$ leads to the following dispersion relation:

$$c=c_r+ic_i=\frac{\mu_1U_1+\mu_2U_2}{\mu_1+\mu_2}-i\frac{e^2}{12(\mu_1+\mu_2)}(\Delta\rho g+\gamma k^2). \quad (10)$$

The wave velocity c_r appears as the mean, weighted this time by the viscosities, of the two fluid velocities. This wave velocity is exactly the velocity of the interface obtained analytically for the full 3D problem of the basic parallel flow.[7] If the viscosities are very different, the wave velocity is twice the bulk velocity of the more viscous fluid $(\mu_1\ll\mu_2\Rightarrow c_r\approx 2U_2\approx 2(\mu_1/\mu_2)\,U_1)$.

Note that as the gravity and the surface tension are stabilizing, the temporal growth rate is always negative and waves are always damped. Indeed, there is no destabilizing term such as inertia in this problem.

C. Kelvin–Helmholtz–Darcy theory

In the two previous linear stability analysis, the viscous terms and the inertia terms have been successively neglected. The linearization of the full Navier–Stokes equation around a basic two-dimensional velocity profile leads to the Orr–Sommerfeld equation. Note that this equation cannot be directly integrated and analytical solutions may be obtained only in some limiting cases:[13] long waves $(k\to 0)$, short waves $(k\to\infty)$ and small Reynolds numbers $(\mathrm{Re}\ll 1)$. However, such analysis only deals with the in plane dissipation and not with the preeminent transverse dissipation existing in the set-up. To take into account this dissipation, we built a new phenomenological equation. Starting from Eq. (1), we take into account the viscous stresses on the two walls in z direction in an equivalent viscous drag force. This forces reads $\mathbf{f}=-\beta\mathbf{u}$ where β is a constant and $\mathbf{u}$ the gap averaged velocity. This modified Navier–Stokes equation, which appears now as a mixing of Euler and Darcy equation, reads as

$$\frac{\partial\mathbf{u}}{\partial t}+(\mathbf{u}.\nabla)\mathbf{u}=-\frac{1}{\rho}\nabla p-\frac{12\nu}{e^2}\mathbf{u}, \quad (11)$$

if we choose $\beta=-12\nu/e^2$ in order to find the Darcy law in the limit of stationary pure viscous flow. Similar equation can be obtained by averaging Navier–Stokes equation through the gap with the assumption of a parabolic velocity profile (Appendix). The same factor β is found but a numerical prefactor (6/5) appears in front of the inertial term. This prefactor has only minor effects.

Equation (11) being a two-dimensional one, it is convenient to introduce the stream function ψ and the equation reduces to

$$\frac{\partial\Delta\psi}{\partial t}+(\mathbf{u}.\nabla)\Delta\psi=-\frac{12\nu}{e^2}\Delta\psi. \quad (12)$$

Small perturbations of the form $\phi(y)\exp[ik(x-ct)]$ superimposed to the basic stationary and unidirectional flow of velocity profile $U_0(y)$ along x direction are governed by the following modified Rayleigh equation:

$$\left(U_0-c-i\frac{12\nu}{ke^2}\right)\left(\frac{d^2\phi}{dy^2}-k^2\phi\right)-\frac{d^2U_0}{dy^2}\phi=0. \tag{13}$$

Solving this modified Rayleigh equation for the discontinuous velocity profile (Fig. 6) and imposing the usual continuity of displacement at the interface $y=0$, the jump condition for the pressure at the interface due to surface tension and the exponential decays at $y=\pm\infty$ leads now to the following dispersion relation:

$$c^2-\left(2\frac{\rho_1U_1+\rho_2U_2}{\rho_1+\rho_2}-i\frac{12(\mu_1+\mu_2)}{(\rho_1+\rho_2)e^2k}\right)c+\frac{\rho_1U_1^2+\rho_2U_2^2}{\rho_1+\rho_2}$$
$$-\frac{\Delta\rho g+\gamma k^2}{(\rho_1+\rho_2)k}-i\frac{12(\mu_1U_1+\mu_2U_2)}{(\rho_1+\rho_2)e^2k}=0. \tag{14}$$

Note that, by contrast to the inviscid case, one cannot change the frame of reference in order to obtain a unique velocity parameter $\Delta U=U_1-U_2$ instead of the two velocities U_1 and U_2. Indeed, the dissipation on the walls kills here the galilean invariance. Since the two velocities are linked by the relation $\mu_1U_1=\mu_2U_2$, we can choose U_1 to be the control parameter and we introduce the ratio $\varepsilon=\mu_1/\mu_2=U_2/U_1$.

The onset of the instability corresponds to $c_i=0$, so to a velocity U_1 which satisfies

$$U_1^2\geqslant\left(\frac{1+\varepsilon}{1-\varepsilon}\right)^2\frac{1}{\rho_1+\rho_2\varepsilon^2}\left(\Delta\rho\frac{g}{k}+\gamma k\right). \tag{15}$$

The critical wave-number is the inverse of the capillary length as in the Kelvin–Helmholtz theory: $k_c=1/l_c=(\Delta\rho g/\gamma)^{1/2}$. The corresponding minimum velocity threshold is then:

$$U_{1_{\min}}=\left[\left(\frac{1+\varepsilon}{1-\varepsilon}\right)^2\frac{2(\Delta\rho g\gamma)^{1/2}}{\rho_1+\rho_2\varepsilon^2}\right]^{1/2}. \tag{16}$$

For $U_1\geqslant U_{1_{\min}}$, the unstable waves are those of wave-numbers in the bandwidth $[k_{\min};k_{\max}]$ of extrema

$$k_{\max/\min}=\frac{\rho_1+\rho_2\varepsilon^2}{2\gamma}\left(\frac{1-\varepsilon}{1+\varepsilon}\right)^2U_1^2$$
$$\pm\left[\left(\frac{\rho_1+\rho_2\varepsilon^2}{2\gamma}\left(\frac{1-\varepsilon}{1+\varepsilon}\right)^2U_1^2\right)^2-\frac{\Delta\rho g}{\gamma}\right]^{1/2}. \tag{17}$$

The wave velocity at the marginal stability ($c_i=0$) is found to be

$$c_r=\frac{\mu_1U_1+\mu_2U_2}{\mu_1+\mu_2}, \tag{18}$$

which is exactly the wave velocity in the pure viscous theory (cf. Eq. (10)).

In the case where the two fluids have very different viscosities as in liquid–gas flow ($\varepsilon\ll1$), Eqs. (16), (17), and (18) reduce to:

$$U_{1_{\min}}\approx\left(\frac{2(\Delta\rho g\gamma)^{1/2}}{\rho_1}\right)^{1/2}, \tag{19}$$

$$k_{\max/\min}\approx\frac{\rho_1}{2\gamma}U_1^2\pm\left[\left(\frac{\rho_1}{2\gamma}U_1^2\right)^2-\frac{\Delta\rho g}{\gamma}\right]^{1/2}, \tag{20}$$

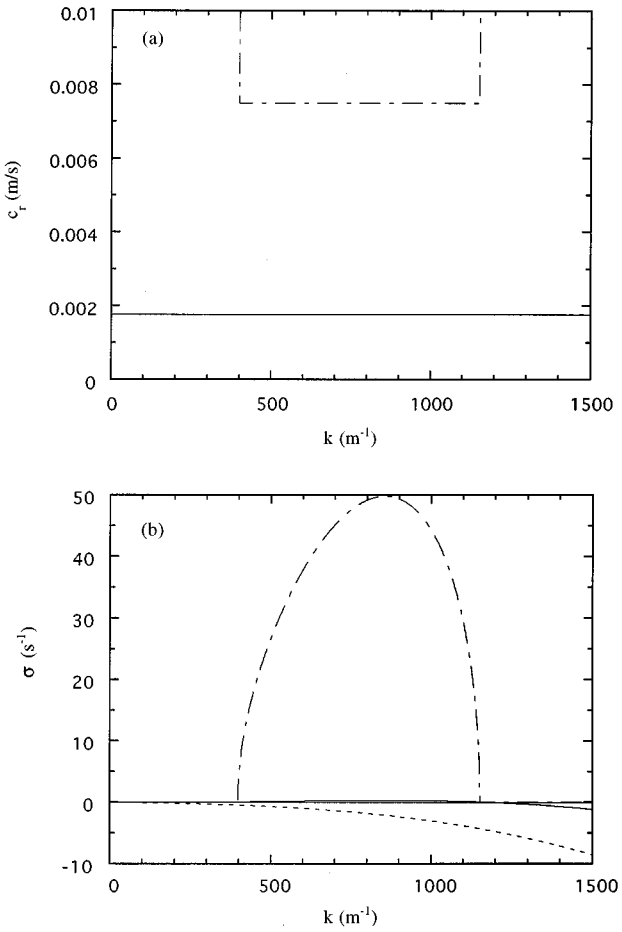

FIG. 7. Theoretical phase wave velocity c_r (a) and temporal growth rate σ (b) as a function of wave-number k for the three different theories: Kelvin–Helmholtz (— - —), Darcy (---), and Kelvin–Helmholtz–Darcy (—) with values of parameters corresponding to the experimental set-up: $U_1=5$ m/s; $\rho_1=1.28$ kg.m^{-3}; $\rho_2=965$ kg.m^{-3}; $\mu_1=1.75\times10^{-5}$ Pa.s; $\mu_2=100\times10^{-3}$ Pa.s; $\gamma=20.6\times10^{-3}$ N/m; $e=0.350$ mm; $g=9.81$ m/s^2.

$$c_r\approx2\frac{\mu_1}{\mu_2}U_1. \tag{21}$$

The expressions of the velocity threshold (Eq. (19)) and of the critical wave-numbers (Eq. 20) are the same as those given by the KH theory when considering $\rho_1\ll\rho_2$ and $U_2\ll U_1$ as for the liquid-gas flow (cf. Eqs. (7) and (8)). By contrast, the wave velocity (Eq. (21)) is the one given by the pure Darcy's theory: It is proportional to the gas velocity and inversely proportional to the viscosity of the liquid. Then the derived ''Kelvin–Helmholtz–Darcy'' (KHD) theory splits the effects of viscosity and inertia: On the one hand, the wave velocity is governed by the viscosity and, on the other hand, the velocity threshold and growing wave-numbers are governed by inertia.

D. Comparison between the theories and the experimental results

The wave velocity c_r and the temporal growth rate σ as a function of the wave-number k given by the three different theories presented above are shown in Fig. 7 for parameter values corresponding to the experiments. The KHD theory

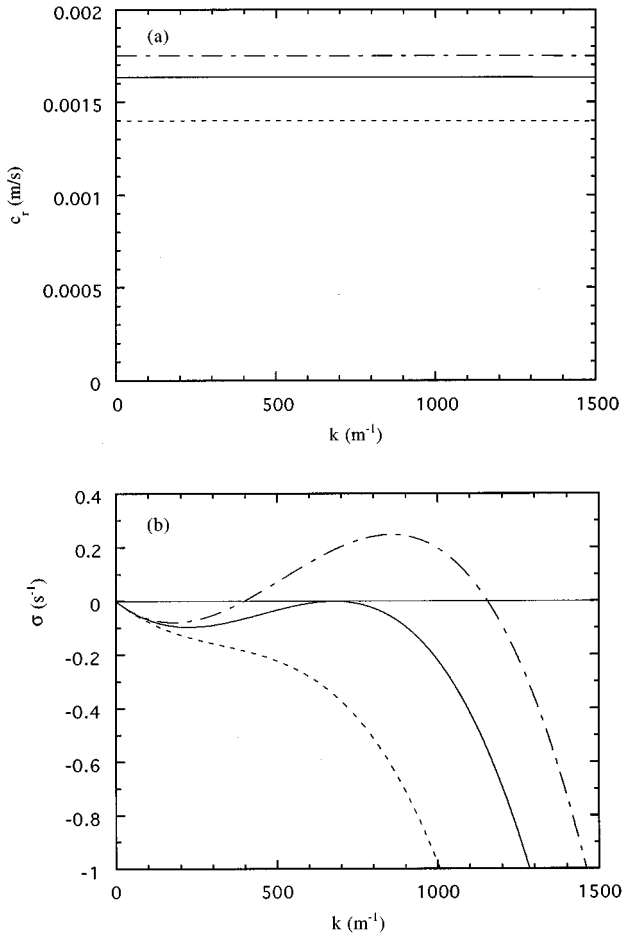

FIG. 8. Phase velocity c_r (a) and temporal growth rate σ (b) as a function of the wavenumber k given by the Kelvin–Helmholtz–Darcy theory for different gas velocity U_1: $U_1=4$ (---), 4.67 (—), and 5 m/s (— - —).

leads to values of wave velocity very near to the ones predicted by Darcy theory so that the two corresponding curves cannot be separated. The KH theory gives much higher values since the friction with the walls is not taken into account in this inviscid theory. The bandwidth of unstable wavenumbers is the same in the KH and KHD theories (Fig. 7(b)) but the temporal growth rate σ is much smaller in the KHD theory than in the KH theory. This can be explained by the dissipation on the walls. For the stable wave-numbers, $\sigma=0$ in the KH theory since the system is non dissipative, but $\sigma<0$ for the Darcy and KHD theories since the corresponding systems are dissipative.

The functions $c_r(k)$ and $\sigma(k)$ given by the KHD theory are shown in Figs. 8(a) and 8(b), respectively, for different values of the air velocity U_1. The threshold is for $U_{1_{\mathrm{KHD}}}\approx 4.67$ m/s which is very close to the experimental threshold of the instability $U_{c_{\mathrm{gas}}}=4.72$ m/s. The phase wave velocity increases linearly with the gas velocity (Fig. 8(a)) and the value at the threshold is $c_{r_{\mathrm{KHD}}}=1.6$ mm/s which is of the order of the experimental value $V_\varphi=1$ mm/s. The temporal growth rate is $\sigma_{\mathrm{KHD}}=-0.35\ \mathrm{s}^{-1}$ at $U_1=4$ m/s and the slope of the growth rate is then $\alpha_{\mathrm{KHD}}=0.5\ \mathrm{m}^{-1}$ which is of the order of the experimental value $\alpha_{\mathrm{exp}}=0.2\ \mathrm{m}^{-1}$. The comparison between the experimental results and the predictions of the KHD theory is quite satisfying. A much more complete comparison dealing with the influence of the thickness and of the liquid viscosity will be reported in a next paper.

IV. CONCLUSION

We have reported results concerning a shear flow instability at the interface between a gas and a liquid in a Hele–Shaw cell. In this high dissipative configuration, the threshold of the instability is surprisingly governed by inertia only, when the wave velocity and the growth rate are both governed by the strong viscous effects. All these experimental results are compatible with a Hopf bifurcation and are well predicted by the linear stability analysis of an equation mixing Euler and Darcy equations. This is the reason why we call the present instability the ''Kelvin–Helmholtz–Darcy'' instability.

ACKNOWLEDGMENTS

We thank Pascal Bérest and Julien de la Gorgue for their help in the preliminary experiments. We are grateful to Vincent Hakim and to Joel Koplik for helpful and stimulating discussions. We are indebted to Olivier Pouliquen and Patrick Huerre for suggesting us the way of adding viscous drag to the Euler equation and to one of the referee for convincing us to present the gap integration in the Appendix.

APPENDIX: GAP AVERAGING OF THE NAVIER–STOKES EQUATION

The KHD analysis was based on Eq. (11) where we modelize the viscous dissipation by adding a viscous drag force to the Euler equation. It is possible to justify this term as presented below.

Starting from Navier–Stokes equation, we assume that there is no transverse velocity and that the two second derivatives in x and y are negligible compared to the z derivative. The equation for the velocity $\mathbf{u}(x,y,z)$ is then

$$\frac{\partial \mathbf{u}}{\partial t}+(\mathbf{u}.\nabla)\mathbf{u}=-\frac{1}{\rho}\nabla p+\nu\frac{\partial^2 \mathbf{u}}{\partial z^2}. \tag{A1}$$

We assume now that the velocity is parabolic in z:

$$\mathbf{u}(x,y,z)=\frac{3}{2}\,\overline{\mathbf{u}}(x,y)\left[1-\left(\frac{2z}{e}\right)^2\right], \tag{A2}$$

where $\overline{\mathbf{u}}(x,y)$ is the gap-averaged velocity as in the usual Darcy's approach. Averaging Eq. (A1) through the gap, we obtain

$$\frac{\partial \overline{\mathbf{u}}}{\partial t}+\frac{6}{5}(\overline{\mathbf{u}}.\nabla)\overline{\mathbf{u}}=-\frac{1}{\rho}\nabla p-\frac{12\nu}{e^2}\,\overline{\mathbf{u}}. \tag{A3}$$

This equation differs from our model Eq. (11) only by the numerical factor 6/5 in front of the inertial term. Similar averaging method has been used in granular layer flow by Savage and Hutter.[19] Solving Eq. (A3) with the discontinuous profile of Fig. 5 leads now to the following dispersion relation:

$$c^2-\left(\frac{11}{5}\frac{\rho_1U_1+\rho_2U_2}{\rho_1+\rho_2}-i\frac{12(\mu_1+\mu_2)}{(\rho_1+\rho_2)e^2k}\right)c+\frac{6}{5}\frac{\rho_1U_1^2+\rho_2U_2^2}{\rho_1+\rho_2}$$
$$-\frac{\Delta\rho g+\gamma k^2}{(\rho_1+\rho_2)k}-i\frac{12(\mu_1U_1+\mu_2U_2)}{(\rho_1+\rho_2)e^2k}=0\,. \tag{A4}$$

The onset of the instability corresponds to a velocity U_1 which satisfies

$$U_1^2\geqslant\frac{5}{2}\frac{(1+\varepsilon)^2}{1-\varepsilon}\frac{1}{3\rho_1-2\rho_1\varepsilon+2\rho_2\varepsilon^2-3\rho_2\varepsilon^3}\left(\Delta\rho\frac{g}{k}+\gamma k\right). \tag{A5}$$

The corresponding critical wave-number is again the inverse of the capillary length $k_c=1/l_c=(\Delta\rho g/\gamma)^{1/2}$ and the corresponding minimum velocity threshold is then

$$U_{1_{\min}}=\left[5\frac{(1+\varepsilon)^2}{1-\varepsilon}\frac{(\Delta\rho g\gamma)^{1/2}}{3\rho_1-2\rho_1\varepsilon+2\rho_2\varepsilon^2-3\rho_2\varepsilon^3}\right]^{1/2}. \tag{A6}$$

For $U_1\geqslant U_{1_{\min}}$, the unstable waves are those of wave-numbers in the bandwidth $[k_{\min};k_{\max}]$ of extrema

$$k_{\max/\min}=\frac{(1-\varepsilon)(3\rho_1-2\rho_1\varepsilon+2\rho_2\varepsilon^2-3\rho_2\varepsilon^3)}{5(1+\varepsilon)^2\gamma}U_1^2$$
$$\pm\left[\left[\frac{(1-\varepsilon)(3\rho_1-2\rho_1\varepsilon+2\rho_2\varepsilon^2-3\rho_2\varepsilon^3)}{5(1+\varepsilon)^2\gamma}U_1^2\right]^2-\frac{\Delta\rho g}{\gamma}\right]^{1/2}. \tag{A7}$$

The wave velocity at the marginal stability ($c_i=0$) is again found to be

$$c_r=\frac{\mu_1U_1+\mu_2U_2}{\mu_1+\mu_2}. \tag{A8}$$

In the case where the two fluids have very different viscosities as in liquid–gas flow ($\varepsilon\ll1$), Eqs. (A6), (A7), and (A8) reduce to:

$$U_{1_{\min}}=\left[\frac{5}{6}\frac{2(\Delta\rho g\gamma)^{1/2}}{\rho_1}\right]^{1/2}, \tag{A9}$$

$$k_{\max/\min}=\frac{3\rho_1}{5\gamma}U_1^2\pm\left[\left(\frac{3\rho_1}{5\gamma}U_1^2\right)^2-\frac{\Delta\rho g}{\gamma}\right]^{1/2}, \tag{A10}$$

$$c_r\approx2\frac{\mu_1}{\mu_2}U_1\,. \tag{A11}$$

The threshold of the instability is then only modified by the factor $\sqrt{5/6}$ when compared to the previous KHD analysis (Eq. (19)). The wave velocity is not changed at all. The band of unstable wave-numbers and so the growth rate are also unchanged when the velocity U_1 is made dimensionless by the critical velocity $U_{1_{\min}}$. Equations (11) and (A3) thus lead to very similar dynamics. Note, that by a convenient rescaling of t and ρ (μ being kept constant), Eq. (A3) is equivalent to Eq. (11) and thus the similarity of the stability analysis of the two equations is not surprising. (We thank Professor G. M. Homsy for pointing out this scaling.)

[1] S. Chandrasekhar, *Hydrodynamic and Hydromagnetic Stability* (Dover, New York, 1961).
[2] J. W. Miles, ''On the generation of surface waves by shear flows,'' J. Fluid Mech. **3**, 185 (1957).
[3] S. A. Thorpe, ''Experiments on the instability of stratified shear flows: immiscible fluids,'' J. Fluid Mech. **39**, 25 (1969).
[4] O. Pouliquen, J.-M. Chomaz, and P. Huerre, ''Propagating Holmboe waves at the interface between two immiscible fluids,'' J. Fluid Mech. **226**, 277 (1994).
[5] M. Rabaud and Y. Couder, ''A shear-flow instability in a circular geometry,'' J. Fluid Mech. **136**, 291 (1983).
[6] P. Barthelet, F. Charru, and J. Fabre, ''Experimental study of interfacial long wave in a two-layer shear flow,'' J. Fluid Mech. **303**, 25 (1995).
[7] P. Gondret, N. Rakotomalala, M. Rabaud, D. Salin, and P. Watzky, ''Viscous parallel flows in finite aspect ratio Hele–Shaw cell: Analytical and numerical results,'' Phys. Fluids **9**, 1841 (1997).
[8] H. J. S. Hele Shaw, ''On the motion of a viscous fluid between two parallel plates,'' Nature (London) **58**, 34 (1898).
[9] H. Darcy, *Les fontaines publiques de la ville de Dijon: distribution d'eau et filtrage des eaux* (Victor Dalmont, Paris, 1856).
[10] J. Bear, *Dynamics of Fluids in Porous Media* (Elsevier, New York, 1972).
[11] S. Orszag, ''Accurate solution of the Orr-Sommerfel stability equation,'' J. Fluid Mech. **50**, 689 (1971).
[12] T. Tatsumi and T. Yoshimura, ''Stability of the laminar flow in a rectangular duct,'' J. Fluid Mech. **212**, 437 (1990).
[13] C. S. Yih, ''Instability due to viscous stratification,'' J. Fluid Mech. **27**, 337 (1967).
[14] T. J. Hanratty, ''Interfacial instabilities caused by air flow over a thin liquid layer,'' in *Waves on Fluid Interfaces* (Academic, New York, 1983).
[15] J. R. D. Francis, ''Wave motions and the aerodynamics drag on a free oil surface,'' Philos. Mag. **45**, 695 (1954).
[16] M. Zeybek and Y. C. Yortsos, ''Long waves in parallel flow in Hele-Shaw cells,'' Phys. Rev. Lett. **67**, 1430 (1991).
[17] M. Zeybek and Y. C. Yortsos, ''Parallel flow in Hele-Shaw cells,'' J. Fluid Mech. **241**, 421 (1992).
[18] H. Lamb, *Hydrodynamics* (Cambridge University Press, Cambridge, 1932), p. 582.
[19] S. B. Savage and K. Hutter, ''The motion of a finite mass of granular materials down a rough incline,'' J. Fluid Mech. **199**, 177 (1989).